

Whole-tumour diffusion kurtosis MR imaging histogram analysis of rectal adenocarcinoma: Correlation with clinical pathologic prognostic factors

Yanfen Cui¹ · Xiaotang Yang¹ · Xiaosong Du¹ · Zhizheng Zhuo² · Lei Xin¹ · Xintao Cheng¹

Received: 26 April 2017 / Revised: 5 September 2017 / Accepted: 25 September 2017 / Published online: 23 October 2017
© European Society of Radiology 2017

Abstract

Objective To investigate potential relationships between diffusion kurtosis imaging (DKI)-derived parameters using whole-tumour volume histogram analysis and clinicopathological prognostic factors in patients with rectal adenocarcinoma.

Material and methods 79 consecutive patients who underwent MRI examination with rectal adenocarcinoma were retrospectively evaluated. Parameters D, K and conventional ADC were measured using whole-tumour volume histogram analysis. Student's t-test or Mann-Whitney U-test, receiver operating characteristic curves and Spearman's correlation were used for statistical analysis.

Results Almost all the percentile metrics of K were correlated positively with nodal involvement, higher histological grades, the presence of lymphangiovascular invasion (LVI) and circumferential margin (CRM) ($p < 0.05$), with the exception of between K_{10th} , K_{90th} and histological grades. In contrast, significant negative correlations were observed between 25th, 50th percentiles and mean values of ADC and D, as well as ADC_{10th} , with tumour T stages ($p < 0.05$). Meanwhile, lower 75th and 90th percentiles of ADC and D values were also correlated inversely with nodal involvement ($p < 0.05$). K_{mean} showed a relatively higher area under the curve (AUC) and higher specificity

than other percentiles for differentiation of lesions with nodal involvement.

Conclusion DKI metrics with whole-tumour volume histogram analysis, especially K parameters, were associated with important prognostic factors of rectal cancer.

Key Points

- K correlated positively with some important prognostic factors of rectal cancer.
- K_{mean} showed higher AUC and specificity for differentiation of nodal involvement.
- DKI metrics with whole-tumour volume histogram analysis depicted tumour heterogeneity.

Keywords Rectal cancer · Diffusion-weighted imaging · Diffusion kurtosis imaging · Prognostic factors · Biomarker

Abbreviations

ADC	Apparent diffusion coefficient
CEA	Carcinoembryonic antigen
CRM	Circumferential margin
CRT	Chemoradiotherapy
D	Diffusivity
DKI	Diffusion kurtosis imaging
DWI	Diffusion weighted imaging
FOV	Field of view
ICC	Interclass correlation coefficient
K	Kurtosis
LVI	Lymphangiovascular invasion
MRI	Magnetic resonance imaging
ROC	Receiver operating characteristic
ROI	Region of interest
SS-EPI	Single shot echo-planar imaging

✉ Xiaotang Yang
yangxt210@126.com

¹ Department of Radiology, Shanxi Province Cancer Hospital, Shanxi Medical University, Taiyuan 030013, China

² MR Clinical Sciences, Philips Healthcare Greater China, Beijing, China

Introduction

Colorectal cancer is one of the leading causes of cancer-related mortality worldwide, while rectal cancer accounts for 30–35 % of these cases [1]. Treatment planning for patients with rectal cancer is primarily based on the risk stratification for local recurrence and distant metastasis. Clinicopathological factors, including TNM staging, histological grade, peritumour lymphovascular invasion (LVI) or neural invasion, circumferential margin (CRM) involvement, and pretreatment serum level of carcinoembryonic antigen (CEA), are widely accepted as powerful prognostic factors, as well as recommended by the National Comprehensive Cancer Network (NCCN) [2–6].

High-spatial-resolution magnetic resonance imaging (MRI) has been widely implemented for local staging of primary rectal cancer prior to treatment [7]. Additionally, functional MRI, such as diffusion-weighted imaging (DWI), has been routinely incorporated into a standard MRI protocol. So far, many investigators have demonstrated the additional value of apparent diffusion coefficients (ADCs) in diagnosis, prognosis and prediction of therapeutic response of rectal cancer [8–10]. However, there have been conflicting conclusions in previous findings regarding ADC values in predicting primary tumour (T) and lymph node (N) staging, as well as histological differentiation grades and LVI status [11–14]. These inconsistent conclusions may be attributed to several factors. On the one hand, owing to the scan parameter differences between DWI sequences (e.g. the different higher b values), measurement variation of ADC (e.g. the difference ROI selection), the mean diffusion parameters are usually unable to depict tumour heterogeneity [15]. On the other hand, conventional DWI is based on Gaussian diffusion behaviour without restriction and ADC is calculated by using a mono-exponential model. However, water molecular diffusion in biological tissue is much more complicated and always restricted due to the presence of microstructures, such as cell membranes and organelles, namely non-Gaussian phenomena [16].

Recently, an advanced non-Gaussian DWI model, diffusion kurtosis imaging (DKI), first proposed by Jensen et al. [17, 18], has been gaining substantial interest because of its subtle reflection of water diffusion in human tissue, thereby providing a more complete characterisation of tissue profile in terms of cellularity and heterogeneity. This model includes both diffusivity and kurtosis parameters. Diffusivity is the diffusion coefficient with correlation of non-Gaussian bias, whereas kurtosis quantifies the deviation of tissue diffusion from Gaussian pattern. Until now, DKI has been widely applied in the assessment of gliomas, prostate cancers, hepatocellular carcinomas and breast lesions, as well as in other organs [19–23].

However, there are few studies of rectal DKI using whole-tumour volume histogram analysis [24, 25], and relationships with clinicopathological prognostic factors were not fully assessed in these studies [26]. Therefore, the purpose of our study was to evaluate the potential association between DKI-

derived parameters and clinicopathological factors in patients with rectal adenocarcinoma by using histogram analysis derived from whole-tumour volumes.

Materials and methods

Patients

Our institutional review board approved this retrospective study and waived the requirement for written informed consent. A series of 162 consecutive patients suspected of having primary rectal carcinoma underwent MRI examination in our hospital between November 2016 and March 2017 were enrolled in the study. Inclusion criteria were as follows: (1) availability of diagnostic-quality preoperative MR images including DKI, (2) without any neoadjuvant therapy before surgical resection, (3) histopathologically confirmed rectal adenocarcinoma, and (4) a time interval between MRI examination and surgery of less than 2 weeks. Clinical information and MR images were retrieved from patient databases. Eighty-three patients were excluded for the following reasons: (1) receiving neoadjuvant chemoradiotherapy (CRT) after initial MRI examination ($n=38$), (2) having distant metastasis ($n=14$) or not having surgical records in our hospital ($n=13$), (3) having other pathological types, such as neuroendocrine carcinoma, melanoma and mucinous adenocarcinoma ($n=11$), (4) those with DKI images with insufficient quality due to severe artefacts ($n=5$), (5) having a time interval between MRI and surgery longer than 2 weeks ($n=2$). Finally, 79 patients with a median age at diagnosis of 60 years (age range, 42–81 years), including 32 (46.0 %) women and 47 (54.0 %) men, were enrolled and analysed in this retrospective study.

MRI protocol

All 79 patients underwent high-resolution MR examination of the rectal area with a 3T system (Achieva; Philips Healthcare, Best, The Netherlands) equipped with an 8-channel phased array torso coils. The standard staging MRI protocol consisted of T_2 -weighted (T_2W) fast spin-echo sequences without fat saturation in three directions. The oblique axial and oblique coronal planes were perpendicular and parallel to the long axis of the tumour as identified on sagittal MRI. The DKI ($b = 0, 700, 1,400, 2,100 \text{ s/mm}^2$) and conventional DWI ($b = 0, 1,000 \text{ s/mm}^2$) sequences were performed in the transverse plane using a single-shot echo-planar imaging (SS-EPI) sequence with identical parameters. The imaging parameters were as follows: TR/TE = 4,000/80 ms; flip angle = 90° ; parallel imaging acceleration factor = 2; slice thickness = 3 mm, no slice gap; field of view (FOV) = 25 cm \times 25 cm; matrix = 256 \times 256; Total imaging time for DKI = 3 min 51 s. The motion-sensitive diffusion gradients were applied in three orthogonal

(X, Y and Z) directions. Patients did not receive any bowel preparation, anti-spasmodic medication, or rectal distention before the MR examination.

Imaging analysis

All functional maps of different parameters were post-processed using an in-house developed software (Matlab, Mathworks, Natick, MA, USA). The in-house software performed a voxel-by-voxel analysis and could automatically output the values per voxel from each region of interest (ROI) measurements. The ADC map was calculated using the standard mono-exponential fit with the equation $S_b/S_0 = \exp(-b \cdot \text{ADC})$, where S_b is the signal intensity at a particular b value and S_0 is signal intensity when b value is 0 s/mm^2 . In the DKI model, the relationship between signal variation and b factors is expressed as: $S_b/S_0 = \exp(-b \cdot D + b^2 \cdot D^2 \cdot K/6)$, D is the diffusion coefficient derived from DKI model, and K is a unitless parameter that signifies the excess kurtosis. Compared with the mono-exponential fit, $K=0$ for perfect Gaussian diffusion and a larger K implies a marked deviation from a perfect Gaussian distribution.

For each patient, two experienced radiologists who were both blinded to all the clinical information and the reference standard (L.X, X.CH., with 10 and 4 years of practice in abdominal imaging, respectively) independently determined the whole-tumour volume by manually drew ROIs along the border of the tumour on each consecutive ADC maps covering the whole lesion, and excluded the cystic, necrosis and haemorrhage areas by referring to the conventional MR images. ROIs were draw with the same criteria on D maps, and were later copied to K maps. The time needed for drawing the ROIs for the whole tumour volume of one patient was approximate 15 min. Each of the ADC, D and K values per pixel from the whole-tumour volume were imported into SPSS Statistics 19.0 (IBM, New York, NY, USA). Various histogram values were then generated, including the 10th, 25th, 50th, mean, 75th and 90th percentile, skewness (a measure of asymmetry of the histogram about its mean) and kurtosis (a measure of the peakedness of the histogram).

Potential prognostic factors

Clinical and histological prognostic factors from the clinical patient database were reviewed. Plasmatic CEA level (ng/ml) at the time of diagnosis was examined. Surgically resected specimens were used to determine the depth of invasion (T stage) and lymph node metastasis (N stage) according to the American Joint Committee on Cancer seventh TNM staging system [27], as well as tumour differentiation grade (well, moderately and poorly differentiated), peritumour LVI or neural invasion, and CRM invasion. LVI, neural invasion and CRM were reported as present or absent.

Statistical analysis

For DKI model fitting, a goodness-of-fit evaluation was performed by using the same dedicated software (Matlab, Mathworks, Natick, MA, USA). The adjusted R^2 value was calculated. All quantitative variables were expressed as means \pm standard deviation (SD) and were tested firstly with the Kolmogorov-Smirnov test for normality analysis. The threshold of CEA was used in our institution. For statistical analysis, Student's t-test or Mann-Whitney U-test were used to assess the differences of all the histogram metrics for the following groups: CEA < 5.0 ng/ml versus ≥ 5.0 ng/ml, pT1–2 versus pT3–4, pN0 versus pN1–2, low grade (G1–2) versus high grade (G3), and the presence versus absence of LVI or neural invasion and the presence versus absence of CRM.

Receiver operating characteristic (ROC) curves were generated to evaluate the diagnostic performance of ADC and DKI histogram metric values for the assessment of prognostic factors. The optimal threshold was chosen according to the Youden index. Differences in performance were analysed by comparing the areas under the ROC curves using the method developed by DeLong et al. [28]. Interobserver agreement for the measurements of the two radiologists was analysed by calculating the interclass correlation coefficient (ICC). An ICC value greater than 0.80 was considered to indicate excellent agreement. Spearman's correlation was performed to evaluate the associations between all the histogram metrics of D , K , ADC and the prognostic factors enrolled in our study. P-values of < 0.05 were considered statistically significant. All statistical analyses were performed using SPSS 19.0 (IBM, New York, NY, USA) and MedCalc 15.8 (MedCalc, Mariakerke, Belgium).

Results

Clinical and histopathological findings

A summary of the prognostic factor distribution in our study population is given in Tables 1 and 2. In brief, there were 32 females (60.81 ± 8.92 years) and 47 males (59.98 ± 9.93 years), with 36 subjects older than 60 years. The average whole tumour volume of rectal cancer is $14.3 \pm 8.4 \text{cm}^3$. At the time of diagnosis, 62 patients had CEA levels lower than 5 ng/ml, while the remaining 17 patients had CEA levels equal to or above 5 ng/ml. According to the analysis of histopathology examination, 29 patients had tumour limited to the rectal muscularis propria (two cases assessed as pT1 and 27 cases as pT2), while the remaining 50 patients were considered to have tumours extending beyond the muscularis propria (36 tumours were pT3 and 14 tumours were pT4). Forty-three patients were staged as N0, whereas 36 patients had metastatic lymph nodes (18 patients had staged pN1 and pN2 tumours,

Table 1 Associations of diffusion-weighted imaging-derived parameters with prognostic factors in histogram analysis

Prognostic factor	n (%)	ADC ($\times 10^{-3}$ mm ² /s)						Skewness	Kurtosis
		mean	10 %	25 %	50 %	75 %	90 %		
CEA level									
≤ 5 ng/ml	62 (78.5)	1.12±0.14	0.81±0.19	0.93±0.21	1.09±0.14	1.30±0.17	1.52±0.25	0.42±0.55	3.45±1.21
> 5 ng/ml	17 (21.5)	1.11±0.20	0.77±0.16	0.92±0.14	1.09±0.20	1.26±0.21	1.42±0.23	0.33±0.71	4.01±1.62
P-value		0.742	0.914 ^a	0.733	0.955	0.429	0.134	0.572	0.373 ^a
pT Stages									
pT1-2	29 (36.7)	1.18±0.19	0.83±0.20	0.98±0.17	1.15±0.19	1.34±0.22	1.56±0.29	0.45±0.52	3.32±1.31
pT3-4	50 (63.3)	1.08±0.11	0.74±0.14	0.89±0.12	1.06±0.11	1.26±0.13	1.47±0.20	0.33±0.51	3.49±1.17
P-value		0.028	0.029 ^a	0.019	0.024	0.072	0.106	0.412	0.513 ^a
pN stages									
pN0	43 (54.4)	1.14±0.16	0.78±0.18	0.93±0.17	1.11±0.16	1.33±0.17	1.56±0.25	0.45±0.64	3.53±1.33
pN1–2	36 (45.6)	1.09±0.16	0.76±0.15	0.91±0.15	1.07±0.15	1.25±0.15	1.44±0.22	0.31±0.53	3.48±1.26
P-value		0.087 ^a	0.381 ^a	0.340 ^a	0.219 ^a	0.047	0.030	0.372	0.951 ^a
Grades									
G1-2	59 (74.7)	1.13±0.15	0.78±0.18	0.93±0.17	1.10±0.16	1.31±0.17	1.53±0.24	0.41±0.53	3.48±1.34
G3	20 (25.3)	1.07±0.14	0.74±0.11	0.89±0.11	1.05±0.13	1.23±0.15	1.45±0.24	0.29±0.51	3.28±0.96
P-value		0.223 ^a	0.152 ^a	0.304	0.206	0.092	0.229	0.392	0.751 ^a
LVI									
Negative	67 (84.8)	1.13±0.15	0.78±0.17	0.93±0.16	1.10±0.14	1.30±0.16	1.52±0.25	0.39±0.47	3.39±1.19
Positive	12 (15.2)	1.06±0.11	0.74±0.07	0.88±0.08	1.05±0.10	1.22±0.13	1.42±0.16	0.24±0.41	3.11±0.63
P-value		0.214 ^a	0.219 ^a	0.325	0.322	0.151	0.199	0.302	0.682 ^a
CRM									
Negative	68 (86.1)	1.14±0.15	0.78±0.18	0.93±0.15	1.10±0.15	1.31±0.16	1.52±0.24	0.40±0.48	3.49±1.13
Positive	11 (13.9)	1.07±0.10	0.74±0.09	0.88±0.07	1.05±0.11	1.23±0.13	1.45±0.18	0.28±0.40	3.25±0.78
P-value		0.205 ^a	0.236 ^a	0.314	0.298	0.113	0.278	0.376	0.584 ^a

respectively). Among all the patients, peritumour LVI was present in 12 patients, CRM was positive in 11 patients, while neural invasion was only present in two patients. For the histological grades, 59 low-grade tumours were classified as G2, and 14 high-grade tumours were classified as G3. However, no tumours were classified as G1.

Interobserver agreement

Overall, the interobserver agreement between two readers was good to excellent for the whole-tumour volume histogram metrics of all ADC, D and K parameters (ICCs ranging from 0.701 to 0.971). Therefore, only results of the first radiologist were used for further analysis. The ICC values for each histogram-based variable parameters are shown in Table 3.

Associations between DKI and ADC parameters and clinicopathological prognostic factors

For all the 79 patients, the mean adjusted R^2 value for the DKI model was 0.96 ± 0.01 (range, 0.94–0.98), indicating the fitting

of tumour diffusion signal decay of rectal cancer by using the non-Gaussian kurtosis model was excellent.

The summary of the histogram metrics of ADC, D and K parameters are provided in Tables 1 and 2. Lower ADC and D values were associated with higher tumour T stage, but significant negative correlations were only observed between the 25th and 50th percentile and mean values of ADC and D, as well as the ADC_{10th}, with the tumour T stages ($r = -0.231\sim -0.284$, all $p < 0.05$). Additionally, the K_{90th} value was significantly higher in tumours with T3-4 than those with T1-2 ($p < 0.05$). Meanwhile, both the 75th and 90th percentiles of ADC and D were correlated inversely with the nodal involvement ($r = -0.234\sim -0.266$, all $p < 0.05$). However, no statistically significant differences or correlations was found for all the ADC or D histogram metrics in tumours of different histological grades and the status of LVI or CRM ($p > 0.05$), although patients with a higher tumour grade or the presence of LVI or CRM had lower ADC or D values. For K parameters, almost all the percentile metrics of K values showed a significant positive correlation with nodal involvement, higher histological grades, the presence of LVI or CRM ($r = 0.236\sim$

Table 2 Associations of diffusion kurtosis imaging (DKI)-derived parameters with prognostic factors in histogram analysis

Prognostic factor	n (%)	mean	10 %	25 %	50 %	75 %	90 %	Skewness	Kurtosis
Diffusion (D, ×10 ⁻³ mm ² /s)									
CEA level									
≤ 5 ng/ml	62 (78.5)	1.23±0.15	0.88±0.18	1.03±0.14	1.20±0.14	1.41±0.17	1.64±0.25	0.41±0.57	3.43±1.24
> 5 ng/ml	17 (21.5)	1.22±0.20	0.92±0.19	1.05±0.20	1.20±0.20	1.37±0.21	1.54±0.23	0.34±0.76	4.03±1.57
P-value		0.527 ^a	0.858 ^a	0.627	0.998	0.440	0.137	0.675	0.159 ^a
pT Stages									
pT1-2	29 (36.7)	1.28±0.20	0.93±0.21	1.09±0.19	1.26±0.19	1.45±0.22	1.67±0.30	0.46±0.58	3.39±1.37
pT3-4	50 (63.3)	1.19±0.11	0.83±0.14	0.99±0.12	1.17±0.12	1.37±0.14	1.58±0.21	0.35±0.60	3.58±1.25
P-value		0.022	0.082 ^a	0.033	0.019	0.115	0.138 ^a	0.474	0.117 ^a
pN stages									
pN0	43 (54.4)	1.26±0.15	0.88±0.18	1.04±0.16	1.22±0.15	1.44±0.17	1.67±0.26	0.45±0.64	3.53±1.33
pN1-2	36 (45.6)	1.19±0.15	0.86±0.16	1.01±0.15	1.18±0.15	1.35±0.16	1.55±0.21	0.31±0.53	3.48±1.26
P-value		0.067 ^a	0.279 ^a	0.201 ^a	0.162 ^a	0.049	0.019^a	0.359	0.937 ^a
Grades									
G1-2	59 (74.7)	1.23±0.16	0.89±0.19	1.04±0.17	1.22±0.16	1.42±0.18	1.63±0.25	0.42±0.62	3.60±1.43
G3	20 (25.3)	1.19±0.14	0.86±0.11	1.00±0.12	1.17±0.14	1.35±0.17	1.57±0.25	0.30±0.58	3.41±1.00
P-value		0.305 ^a	0.294 ^a	0.318	0.255	0.159 ^a	0.322	0.435	0.701 ^a
LVI									
Negative	67 (84.8)	1.24±0.16	0.87±0.18	1.03±0.17	1.21±0.16	1.41±0.18	1.63±0.26	0.42±0.60	3.53±1.37
Positive	12 (15.2)	1.18±0.11	0.84±0.08	1.00±0.09	1.17±0.11	1.34±0.14	1.54±0.16	0.22±0.57	3.39±0.72
P-value		0.444 ^a	0.585 ^a	0.477	0.485	0.292	0.357	0.641	0.539 ^a
CRM									
Negative	68 (86.1)	1.23±0.16	0.87±0.17	1.04±0.17	1.22±0.15	1.42±0.17	1.63±0.25	0.42±0.60	3.53±1.37
Positive	11 (13.9)	1.18±0.12	0.85±0.08	1.00±0.10	1.17±0.11	1.34±0.14	1.55±0.17	0.22±0.57	3.39±0.72
P-value		0.457 ^a	0.593 ^a	0.327	0.373	0.132	0.258	0.641	0.539 ^a
Kurtosis (K)									
CEA level									
≤ 5 ng/ml	62 (78.5)	0.92±0.09	0.67±0.17	0.81±0.10	0.93±0.09	1.04±0.09	1.15±0.11	-0.28±1.02	4.88±2.92
> 5 ng/ml	17 (21.5)	0.95±0.10	0.69±0.11	0.83±0.08	0.95±0.08	1.07±0.11	1.20±0.18	-0.29±1.26	5.32±3.19
P-value		0.216	0.924 ^a	0.424	0.351	0.165	0.135	0.973	0.694 ^a
pT Stages									
pT1-2	29 (36.7)	0.92±0.09	0.66±0.15	0.81±0.11	0.93±0.08	1.03±0.08	1.13±0.11	-0.41±1.02	5.10±2.82
pT3-4	50 (63.3)	0.94±0.10	0.68±0.17	0.82±0.09	0.94±0.10	1.06±0.11	1.21±0.17	-0.29±1.13	4.78±3.23
P-value		0.321	0.535 ^a	0.779	0.721	0.269	0.039	0.166	0.286 ^a
pN stages									
pN0	43 (54.4)	0.89±0.09	0.63±0.16	0.78±0.10	0.90±0.09	1.02±0.09	1.13±0.12	-0.39±0.88	4.43±2.34
pN1-2	36 (45.6)	0.97±0.08	0.72±0.15	0.86±0.08	0.97±0.07	1.08±0.09	1.20±0.14	-0.16±1.26	5.64±3.49
P-value		0.000	0.004^a	0.000	0.001^a	0.011^a	0.015	0.335	0.082 ^a
Grades									
G1-2	59 (74.7)	0.91±0.09	0.66±0.16	0.80±0.10	0.92±0.09	1.03±0.09	1.14±0.12	-0.31±0.92	4.59±2.57
G3	20 (25.3)	0.97±0.10	0.71±0.16	0.86±0.09	0.97±0.08	1.09±0.10	1.21±0.16	-0.20±1.45	6.12±3.75
P-value		0.012	0.152 ^a	0.025	0.011	0.017	0.155 ^a	0.737	0.064 ^a
LVI									
Negative	67 (84.8)	0.91±0.09	0.65±0.16	0.80±0.10	0.92±0.09	1.03±0.10	1.15±0.11	-0.39±0.88	4.43±2.34
Positive	12 (15.2)	1.00±0.07	0.77±0.08	0.89±0.08	1.00±0.07	1.10±0.08	1.22±0.07	-0.16±1.26	5.64±3.49
P-value		0.003	0.011^a	0.004	0.002	0.019	0.041	0.293	0.315 ^a
CRM									
Negative	68 (86.1)	0.91±0.09	0.65±0.15	0.80±0.09	0.92±0.09	1.03±0.09	1.14±0.11	-0.38±0.87	4.44±2.33
Positive	11 (13.9)	1.00±0.06	0.76±0.07	0.88±0.08	0.99±0.06	1.10±0.09	1.22±0.08	-0.16±1.24	5.65±3.47
P-value		0.002	0.015^a	0.005	0.002	0.021	0.036	0.342	0.346 ^a

Note. D is the diffusion coefficient derived from DKI model, and K is a unitless parameter that signifies the excess kurtosis

0.406, all $p < 0.05$), with the exception of between K_{10th} , K_{90th} and histological grades ($r = 0.161$ and 162 , both $P > 0.05$) (Figs. 1 and 2). Regarding the CEA level, none of the ADC and DKI histogram metrics had significant discriminative power in this study. Likewise, no correlation was observed between the skewness or kurtosis values of ADC, D, K and all the prognostic factors enrolled in our study ($p > 0.05$).

Diagnostic performance of DKI and ADC histogram parameters

Table 4 demonstrates the results of the ROC analysis of the multi-parametric imaging measures for the detection of patients with metastatic lymph nodes. For all the histogram metrics, both the 75th and 90th percentiles of ADC and D, as well as all the percentiles of K values, exhibited significant

Table 3 Interobserver agreement for whole-tumour volume

Histogram metrics	ADC	D	K
Mean	0.934 (0.833–0.975)	0.963 (0.905–0.981)	0.971 (0.949–0.991)
10th	0.864 (0.731–0.936)	0.883 (0.736–0.947)	0.915 (0.886–0.970)
25th	0.926 (0.893–0.965)	0.933 (0.893–0.954)	0.949 (0.897–0.971)
50th	0.941 (0.913–0.978)	0.965 (0.935–0.981)	0.983 (0.953–0.993)
75th	0.892 (0.813–0.947)	0.904 (0.845–0.957)	0.935 (0.891–0.959)
90th	0.866 (0.735–0.913)	0.889 (0.786–0.931)	0.921 (0.834–0.965)
Skewness	0.701 (0.495–0.839)	0.715 (0.735–0.913)	0.736 (0.535–0.853)
Kurtosis	0.731 (0.523–0.855)	0.746 (0.537–0.869)	0.778 (0.597–0.897)

Note. Data are interobserver correlation coefficients, with 95 % confidence intervals in brackets

D is the diffusion coefficient derived from diffusion kurtosis imaging (DKI) model, and K is a unitless parameter that signifies the excess kurtosis

discriminative power for nodal involvement ($p < 0.05$). Regarding the comparison of diagnostic performance between them, the AUC for K_{mean} value was higher than those of other histogram metrics, but did not reach a significant level ($p > 0.05$). The specificity (88.37 %) was higher than that of other histogram metrics with a threshold of 0.893 for K_{mean} (Fig. 3).

Discussion

In the present study, we successfully performed DKI using whole-tumour volume measurement in a reproducible manner by different readers, and then found that DKI-derived K was significantly correlated with some prognostic factors for rectal

cancer, including lymph node status, histological grade and the presence of LVI or CRM. Meanwhile, ADC and D were significantly correlated with tumour T stages and lymph node status. Therefore, DKI-derived histogram metrics may indeed be a powerful non-invasive imaging biomarker of tumour aggressiveness in rectal cancer. Application of the DKI model in body imaging has been gaining increasing interest in recent years [22, 24, 26, 29]. Although still with many unconfirmed aspects, such as the optimal number, range and maximum value of b factors, the DKI model seems to be the preferred model in terms of model fit and repeatability [30]. It is suggested that at least three b values with a maximum value somewhat larger, approximately $2,000 \text{ s/mm}^2$, be used for clinical practice in body imaging [16]. For previous studies

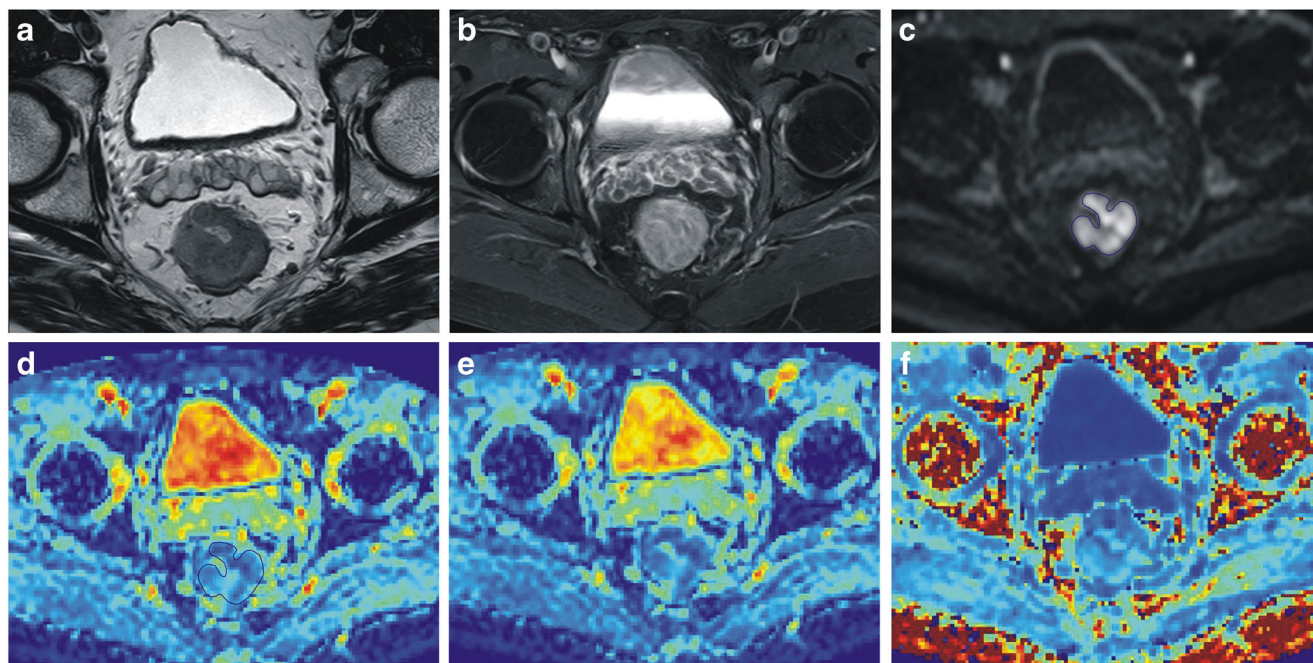
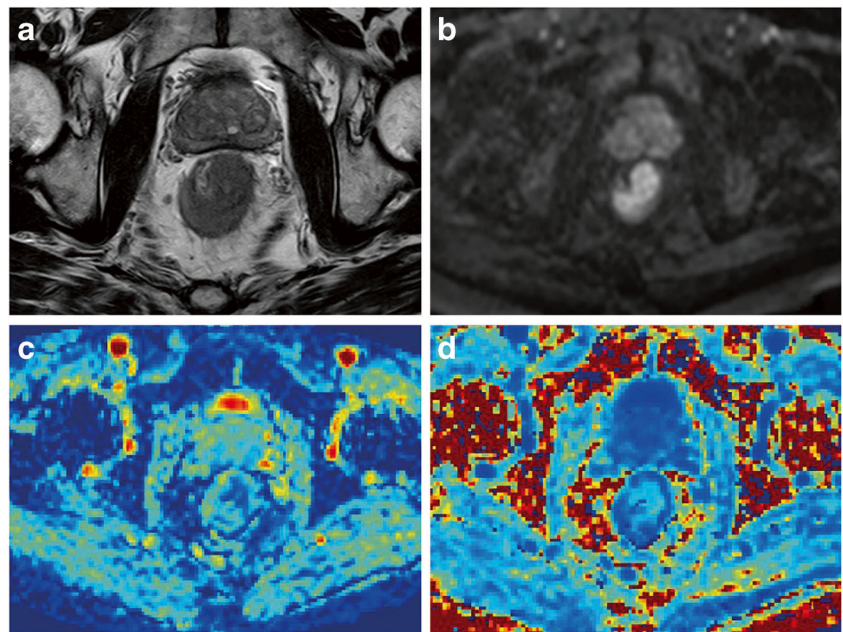


Fig. 1 MR images of a 56-year-old man with poorly differentiated rectal cancer. Axial T2-weighted MR (A) and contrast T1-weighted MR image (B) show a mass occupying more than three-quarters of the rectal wall, with mild enhancement. (C) High b-value ($1,400 \text{ s/mm}^2$) diffusion-

weighted image shows a hyperintense tumour. The color-coded ADC map (D), D map (E) and K map (F) show heterogeneous blue in the corresponding tumour with ADC of $0.911 \times 10^{-3} \text{ s/mm}^2$, D_{mean} of $1.035 \times 10^{-3} \text{ s/mm}^2$ and K_{mean} value of 0.916

Fig. 2 MR images of a 71-year-old man with moderately differentiated rectal cancer. Axial T2-weighted MR image (A) shows a mass occupying more than three-quarters of the rectal wall. (B) High b-value (1,400 s/mm²) diffusion-weighted image shows a hyperintense tumour. The color-coded D map (C) and K map (D) shows heterogeneous blue in the corresponding tumour with a D_{mean} of 1.162 × 10⁻³ s/mm² and K_{mean} value of 0.863



of DKI in rectal cancer, the b value spectrum was mostly 0–2 100 s/mm², as high b values can reduce the apparent departure from linearity of the diffusion kurtosis. In our present study, we chose four b values with 0, 700, 1,400 and 2,100 s/mm² in accordance with previous studies [26].

It has been demonstrated that significantly higher K values were found in patients with high-grade tumours in a number of

studies [22, 31, 32]. Similar results were found in our study, where almost all the percentile metrics of K exhibited significantly positive correlations for tumours with higher histological grade, as well as for tumours with metastatic lymph nodes or the presence of LVI or CRM. Additionally, K_{90th} was also significantly higher in patients with a higher T stage. This is an interesting finding as it has been proven that all these indexes are

Table 4 Diagnostic Performance of diffusion kurtosis imaging (DKI) and ADC histogram metrics using whole-tumour volume Analysis for the detection of nodal involvement

Parameters	Threshold	AUC	Sensitivity (%)	Specificity (%)	P-value
ADC _{mean}	≤1.191	0.612 (0.488–0.737)	91.67 (77.5–98.2)	34.88 (21.0–50.9)	0.079
ADC _{10th}	≤0.804	0.557 (0.441–0.669)	72.22 (54.8–85.8)	48.84 (33.3–64.5)	0.379
ADC _{25th}	≤1.057	0.563 (0.446–0.674)	97.22 (85.5–99.9)	23.26 (11.8–38.6)	0.337
ADC _{50th}	≤1.058	0.581 (0.464–0.691)	61.11 (43.5–76.9)	62.79 (46.7–77.0)	0.215
ADC _{75th}	≤1.354	0.636 (0.520–0.741)	80.56 (64.0–91.8)	46.51 (31.2–62.3)	0.032
ADC _{90th}	≤1.538	0.652 (0.537–0.756)	80.56 (64.0–91.8)	51.16 (35.5–66.7)	0.015
D _{mean}	≤1.191	0.620 (0.504–0.727)	55.56 (77.5–98.2)	69.77 (21.0–50.9)	0.059
D _{10th}	≤0.904	0.571 (0.455–0.682)	66.67 (49.0–81.4)	53.49 (37.7–68.8)	0.276
D _{25th}	≤1.158	0.584 (0.468–0.694)	97.22 (85.5–99.9)	23.26 (11.8–38.6)	0.194
D _{50th}	≤1.162	0.592 (0.475–0.701)	58.33 (40.8–74.5)	65.12 (49.1–79.0)	0.157
D _{75th}	≤1.428	0.639 (0.523–0.744)	69.44 (51.9–83.7)	60.47 (44.4–75.0)	0.028
D _{90th}	≤1.630	0.654 (0.539–0.758)	75.00 (57.8–87.9)	58.14 (42.1–73.0)	0.014
K _{mean}	>0.979	0.735 (0.624–0.828)	55.56 (38.1–72.1)	88.37 (74.9–96.1)	0.000
K _{10th}	>0.688	0.691 (0.577–0.790)	75.00 (57.8–87.9)	58.14 (42.1–73.0)	0.002
K _{25th}	>0.809	0.731 (0.619–0.824)	72.22 (54.8–85.8)	65.12 (49.1–79.0)	0.000
K _{50th}	>0.894	0.728 (0.616–0.822)	91.67 (77.5–98.2)	46.51 (31.2–62.3)	0.000
K _{75th}	>0.985	0.666 (0.551–0.768)	88.89 (73.9–96.9)	39.53 (25.0–55.6)	0.007
K _{90th}	>1.079	0.648 (0.533–0.752)	86.11 (70.5–95.3)	41.86 (27.1–57.9)	0.017

Note. 95 % confidence intervals in bracket

D is the diffusion coefficient derived from the diffusion kurtosis imaging (DKI) model, and K is a unitless parameter that signifies the excess kurtosis

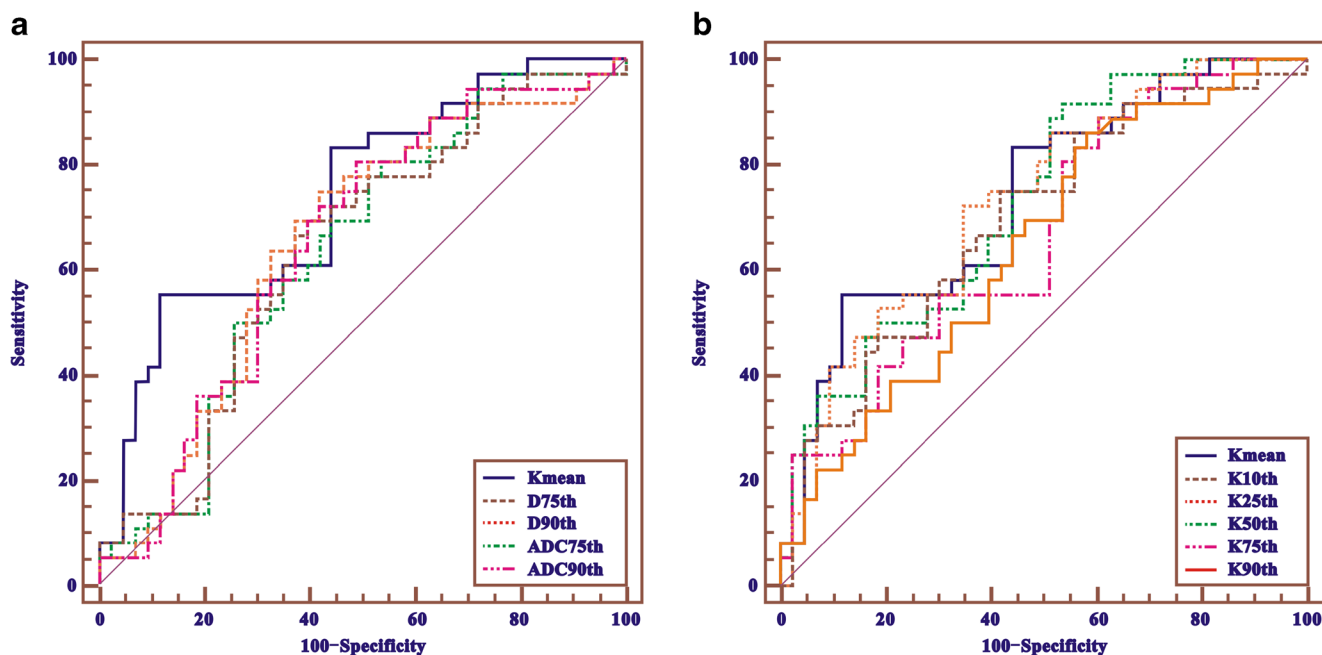


Fig. 3 A comparison of the diagnostic ability for distinguishing nodal involvement between histogram ADC, D and K. Receiver operating characteristic curve analysis shows that the K_{mean} had a higher area

under the curve (0.735) than that of the others, but did not reach a significant level, compared with the 75th and 90th percentiles of ADC and D (A), as well as all the percentiles of K values (B)

powerful predictors of local recurrence and distant metastases, suggesting that a higher K value in itself correlates with poor prognosis. This could be explained by the fact that K values are indirectly derived from the microstructure complexity of the tumour [17], and may thus reflect the aggressiveness of the tumour tissue profile. The increased cellular density, larger percentage of gland formation and marked variation of nuclear pleomorphism within more aggressive rectal cancer were associated with increasing tissue complexity at the microstructural level, resulting in higher kurtosis of K values.

On the other hand, there was a similar trend toward lower ADC and D values for patients with all the above in their histopathological index, although statistical significance was mainly found between 25th and 50th percentages and mean values of ADC or D and tumour T stages, as well as between the 75th and 90th percentile metrics of ADC or D and tumour N stages. It can be explained that the D value, a corrected ADC value, may actually reflect the water molecular diffusion accounting for non-Gaussian diffusion behaviour, which has a similar physical meaning to ADC derived from the mono-exponential model. However, there was no correlation between any DKI or DWI parameters and CEA levels, suggesting that the pretreatment CEA level might not reflect the actual status of the rectal cancer.

Patients with positive nodal status may have an indication for neoadjuvant CRT or extended pelvic surgery. However, reliable detection of metastatic lymph nodes, a main prognostic indicator of distant metastasis and unfavourable survival, is still a challenge in diagnostic imaging of rectal cancer [33].

ROC curve analysis in our study showed both the DKI and DWI parameters of rectal cancer may provide important indicators of lymph node status, thereby improving tumour N staging prior to therapy. By comprehensive comparison of histogram D, K and ADC, we found that K_{mean} showed the highest specificity with the highest AUC than other histogram metrics, although without a significant difference, further validating the superiority of non-Gaussian distribution model. Some investigators found that pretreatment ADC is significantly different in metastatic lymph node [11, 12], which is not consistent with results from others [14, 34]. These inconsistent results between the reported studies may be due to the relatively small patient population and imbalanced population distribution. Another reason could be that differences in measuring techniques, such as whole-tumour volume ROIs rather than smaller oval-shaped ROIs, may result in different outcomes [15]. It is well known that rectal cancer is heterogeneous, even within the same histological type. The difference in percentiles of quantitative metrics derived from DKI and DWI for various subtypes in our study demonstrated this phenomenon. Additionally, we excluded the extreme values of histogram indices, such as minimum and maximum values, because they are subject to measuring errors.

Our study had several limitations. First, as a retrospective study, there was unavoidable selection bias, because many patients presenting with locally advanced rectal cancers underwent neoadjuvant therapy, limiting our study population. Second, the relatively small sample size and imbalanced population distribution within some subtypes also limits the

applicability of results. Thus, large prospective, multi-institutional cohort studies with a greater statistical power are necessary to further validate the results of the present study. Third, we did not compare the relationship between DKI parameters with the immunohistochemical features of rectal cancer, such as proliferative Ki-67 index, as integration of some immunohistochemical features into risk stratification schemes may be useful in clinical practices.

In conclusion, our study demonstrated that DKI metrics with whole-tumour volume histogram analysis, especially the K parameters, were associated with important prognostic factors of rectal cancer. Further investigation is required to determine whether DKI metrics are useful as imaging biomarkers in predicting the biological properties of rectal cancer in clinical practice.

Funding This work was supported by the fund of Science and Technology Project of Shanxi Province (No. 20150313007-5).

Compliance with ethical standards

Guarantor The scientific guarantor of this publication is Xiaotang Yang.

Conflict of interest The authors of this manuscript declare no relationships with any companies whose products or services may be related to the subject matter of the article.

Statistics and biometry No complex statistical methods were necessary for this paper.

Informed consent Written informed consent was waived by the Institutional Review Board.

Ethical approval Institutional Review Board approval was obtained.

Methodology

- retrospective
- diagnostic or prognostic study
- performed at one institution

References

1. Lee YC, Hsieh CC, Chuang JP (2013) Prognostic significance of partial tumor regression after preoperative chemoradiotherapy for rectal cancer: a meta-analysis. *Dis Colon Rectum* 56:1093–1101
2. Boras Z, Kondza G, Sisljagic V et al (2012) Prognostic factors of local recurrence and survival after curative rectal cancer surgery: a single institution experience. *Coll Antropol* 36:1355–1361
3. Cienfuegos JA, Rotellar F, Baixauli J et al (2015) Impact of perineural and lymphovascular invasion on oncological outcomes in rectal cancer treated with neoadjuvant chemoradiotherapy and surgery. *Ann Surg Oncol* 22:916–923
4. Lee JH, Jang HS, Kim JG et al (2012) Lymphovascular invasion is a significant prognosticator in rectal cancer patients who receive preoperative chemoradiotherapy followed by total mesorectal excision. *Ann Surg Oncol* 19:1213–1221
5. Peng J, Sheng W, Huang D et al (2011) Perineural invasion in pT3N0 rectal cancer: the incidence and its prognostic effect. *Cancer* 117:1415–1421
6. Madbouly KM, Abbas KS, Hussein AM (2014) Metastatic lymph node ratio in stage III rectal carcinoma is a valuable prognostic factor even with less than 12 lymph nodes retrieved: a prospective study. *Am J Surg* 207:824–831
7. Zhang XM, Zhang HL, Yu D et al (2008) 3-T MRI of rectal carcinoma: preoperative diagnosis, staging, and planning of sphincter-sparing surgery. *AJR Am J Roentgenol* 190:1271–1278
8. Blazic IM, Lilic GB, Gajic MM (2017) Quantitative Assessment of Rectal Cancer Response to Neoadjuvant Combined Chemotherapy and Radiation Therapy: Comparison of Three Methods of Positioning Region of Interest for ADC Measurements at Diffusion-weighted MR Imaging. *Radiology* 282:418–428
9. Choi MH, Oh SN, Rha SE et al (2016) Diffusion-weighted imaging: Apparent diffusion coefficient histogram analysis for detecting pathologic complete response to chemoradiotherapy in locally advanced rectal cancer. *J Magn Reson Imaging* 44:212–220
10. Cai PQ, Wu YP, An X et al (2014) Simple measurements on diffusion-weighted MR imaging for assessment of complete response to neoadjuvant chemoradiotherapy in locally advanced rectal cancer. *Eur Radiol* 24:2962–2970
11. Curvo-Semedo L, Lambregts DM, Maas M et al (2012) Diffusion-weighted MRI in rectal cancer: apparent diffusion coefficient as a potential noninvasive marker of tumor aggressiveness. *J Magn Reson Imaging* 35:1365–1371
12. Akashi M, Nakahusa Y, Yakabe T et al (2014) Assessment of aggressiveness of rectal cancer using 3-T MRI: correlation between the apparent diffusion coefficient as a potential imaging biomarker and histologic prognostic factors. *Acta Radiol* 55:524–531
13. Tong T, Yao Z, Xu L et al (2014) Extramural depth of tumor invasion at thin-section MR in rectal cancer: associating with prognostic factors and ADC value. *J Magn Reson Imaging* 40:738–744
14. Sun Y, Tong T, Cai S et al (2014) Apparent Diffusion Coefficient (ADC) value: a potential imaging biomarker that reflects the biological features of rectal cancer. *PloS one* 9:e109371
15. Lambregts DM, Beets GL, Maas M et al (2011) Tumor ADC measurements in rectal cancer: effect of ROI methods on ADC values and interobserver variability. *Eur Radiol* 21:2567–2574
16. Rosenkrantz AB, Padhani AR, Chenevert TL et al (2015) Body diffusion kurtosis imaging: Basic principles, applications, and considerations for clinical practice. *J Magn Reson Imaging* 42:1190–1202
17. Jensen JH, Helpert JA, Ramani A et al (2005) Diffusional kurtosis imaging: the quantification of non-gaussian water diffusion by means of magnetic resonance imaging. *Magn Reson Med* 53:1432–1440
18. Jensen JH, Helpert JA (2010) MRI quantification of non-Gaussian water diffusion by kurtosis analysis. *NMR Biomedicine* 23:698–710
19. Pang H, Ren Y, Dang X et al (2016) Diffusional kurtosis imaging for differentiating between high-grade glioma and primary central nervous system lymphoma. *J Magn Reson Imaging* 44:30–40
20. Bai Y, Lin Y, Tian J et al (2016) Grading of Gliomas by Using Monoexponential, Biexponential, and Stretched Exponential Diffusion-weighted MR Imaging and Diffusion Kurtosis MR Imaging. *Radiology* 278:496–504
21. Goshima S, Kanematsu M, Noda Y et al (2015) Diffusion kurtosis imaging to assess response to treatment in hypervascular hepatocellular carcinoma. *AJR Am J Roentgenol* 204:W543–W549
22. Wang Q, Li H, Yan X et al (2015) Histogram analysis of diffusion kurtosis magnetic resonance imaging in differentiation of pathologic Gleason grade of prostate cancer. *Urol Oncol* 33(337):e15–e24
23. Nogueira L, Brandao S, Matos E et al (2014) Application of the diffusion kurtosis model for the study of breast lesions. *Eur Radiol* 24:1197–1203

24. Yu J, Xu Q, Song JC, et al (2016) The value of diffusion kurtosis magnetic resonance imaging for assessing treatment response of neoadjuvant chemoradiotherapy in locally advanced rectal cancer. *Eur Radiol* 1–10
25. Yu J, Huang DY, Li Y et al (2016) Correlation of standard diffusion-weighted imaging and diffusion kurtosis imaging with distant metastases of rectal carcinoma. *J Magn Reson Imaging* 44:221–229
26. Zhu L, Pan Z, Ma Q, et al (2016) Diffusion Kurtosis Imaging Study of Rectal Adenocarcinoma Associated with Histopathologic Prognostic Factors: Preliminary Findings. *Radiology* 160094.
27. Edge SB, Compton CC (2010) The American Joint Committee on Cancer: the 7th edition of the AJCC cancer staging manual and the future of TNM. *Annals of surgical oncology* 17:1471–1474
28. DeLong ER, DeLong DM, Clarke-Pearson DL (1988) Comparing the areas under two or more correlated receiver operating characteristic curves: a nonparametric approach. *Biometrics* 44:837–845
29. Li HM, Zhao SH, Qiang JW, et al (2017) Diffusion kurtosis imaging for differentiating borderline from malignant epithelial ovarian tumors: A correlation with Ki-67 expression. *J Magn Reson Imaging*
30. Jambor I, Merisaari H, Taimen P et al (2015) Evaluation of different mathematical models for diffusion-weighted imaging of normal prostate and prostate cancer using high b-values: a repeatability study. *Magn Reson Med* 73:1988–1998
31. Sun K, Chen X, Chai W et al (2015) Breast Cancer: Diffusion Kurtosis MR Imaging-Diagnostic Accuracy and Correlation with Clinical-Pathologic Factors. *Radiology* 277:46–55
32. Van Cauter S, Veraart J, Sijbers J et al (2012) Gliomas: diffusion kurtosis MR imaging in grading. *Radiology* 263:492–501
33. Al-Sukhni E, Milot L, Fruitman M et al (2012) Diagnostic accuracy of MRI for assessment of T category, lymph node metastases, and circumferential resection margin involvement in patients with rectal cancer: a systematic review and meta-analysis. *Ann Surg Oncol* 19: 2212–2223
34. Attenberger UI, Pilz LR, Morelli JN et al (2014) Multi-parametric MRI of rectal cancer - do quantitative functional MR measurements correlate with radiologic and pathologic tumor stages? *Eur J Radiol* 83:1036–1043